한국지반환경공학회 논문집 제6권 제5호 2006년 10월 pp. 79~87

A Numerical Study on Dispersion of Inert Particles in a Rough Single Fracture

거친 균열 암반에서의 용질 입자 확산에 대한 수치적 연구

정우창*

Jeong, Woochang*

Abstract

This paper presents the numerical model developed to simulate the solute transport in rough and smooth single fractures. The roughness of these fractures is represented by using the fractal surface method. In this study, the 3D transport model, which is based on the random walk technique, is used to simulate the dispersion process of a solute which is represented by numerical particles. As the simulation results, it can be observed that the dispersion of solute in the fracture is significantly affected by the fracture roughness and particle size.

Keywords : Solute Transport, Random walk model, Fracture roughness

요 지

본 논문은 매끄럽거나 거친 단일 균열에서의 용질 이동을 모의하기 위해 개발된 수치모형을 통해 용질 입자의 확산에 수치적 연구를 수행한 것이다. 단일 균열의 조도는 프랙탈 방법을 통해 표현되었으며, 본 연구에서 사용된 3차원 이동 모형은 random walk 기법에 근거하여 개발하였다. 모의실험 결과 단일 균열내에서의 용질 입자의 확산은 균열의 조도와 입자의 크기에 큰 영향을 받는 것으로 나타났다.

주요어 : 용질 이동, random walk 모형, 균열 조도

* Member, Senior Researcher, Water Resources and Environmental Research Center, Korea Institute of Water and Environment, Korea Water Resources Corporation(jeongwc@kwater.or.kr)

1. Introduction

We consider in this paper the different cases of the conservative and non-conservative solute transport in a smooth or rough fracture (Fleurant, 2000). In the case of a single fracture, the solute transport can be treated to two-dimensional or three-dimensional problem (Neretnieks et al., 1982; Novakowski et al., 1985). In two-dimensional problem, it can be supposed that the fluid flows with constant velocity, and in three-dimensional problem it is necessary to introduce a parabolic velocity profile on the section of the fracture (Figure 1). In a single fracture, the transport processes consist of the convection in the longitudinal direction and the molecular diffusion in the vertical direction. In general, this is called as Taylor dispersion (Kinzelbach, 1986).

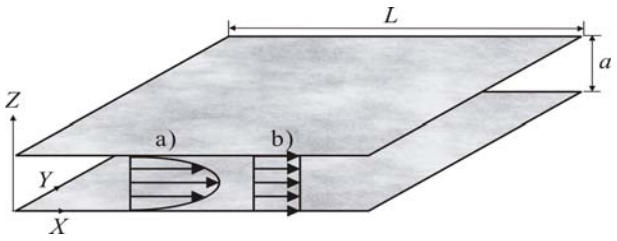

Figure 1. Velocity profile in a single fracture: a) 3D case and b) 2D case.

In a smooth fracture, when $L[m]$ is the length of the fracture and $U[m/s]$ is the mean velocity of the fluid, Hull et al. (1987) give several indications on the conditions of the transport by introducing the concept of Fickian process for the solute transport: if the mean residence time is smaller than the critical time $\left(\frac{6a^2}{\pi^2 D_m}\right)$, where $D_m[m^2/s]$ is the molecular diffusion and $a[m]$ is the aperture, the transport is thus non Fickian and this non Fickian transport is often argued to be results of heterogeneities that can be ignored. On the contrary case, when the molecular diffusion is dominant and makes a homogeneity of the concentration of a tracer in the aperture of the fracture, the transport is thus Fickian and is modeled by using the classical convection-dispersion equation. The coefficient of the longitudinal dispersion can be written as (Aris, 1956):

$$D_X = D_m + \frac{U^2 a^2}{210 D_m} \tag{1}$$

This coefficient of dispersion, which is called as Taylor-Aris coefficient, has a asymptotic value and is valuable only from the critical length of the fracture (Kessler and Hunt, 1994).

In the case of three-dimensional transport, the local particle velocities can be determined with Poiseuille's velocity profile that the liquid in the center is moving fastest while the liquid touching the walls of the tube is stationary due to friction:

$$U_X(Z) = \frac{3}{2} U\left(1 - \frac{4z^2}{a^2}\right) \tag{2}$$

This profile represents that the velocity is zero at the fracture walls and is maximum $\left(\frac{3}{2}U\right)$ at the center of the fracture.

If the residence time of particles is smaller than the critical time, it is necessary to be treated as a three-dimensional problem (that is the parabolic distribution of velocity must be considered). However, in the contrary case, it can be simplified to two-dimensional problem (that is, the Taylor-Aris dispersion is used).

2. Models

2.1 Generation of rough single fracture

In order to simulate the particle transport in a rough single fracture, first of all, it is necessary to generate the roughness of the fracture. The method

used for rough fractures in this study is the fractal surface theory and is written in detail in Brown (1995) and Jeong (2000).

The procedure for the generation of a rough fracture is as follow: Firstly, two fractal surfaces with the same mean and standard deviation are generated and secondly, the aperture (the distance a between two fractal surfaces in Figure 1) of this fracture is needed to define. As the aperture is diminished, the contact areas between two fracture surfaces may be appeared. This contact areas are the function of the effective normal stress applied to the single fracture. Figure 2 shows a fracture generated with the fractal dimension (D) of 2.5, the mean and standard deviation of fractal surface roughness are $0.1mm$ and $0.05mm$, respectively and the mean aperture is $8mm$.

2.2 Flow model

In order to apply the random walk model to solute particle, it needs to determine the velocities $u_X(Z)$ and u_Y at each cell of the grid. Once the variable apertures are generated in a rough single fracture which is discretized into square grids and each cell of size e being characterized by its own aperture a, the local flow can be calculated by taking the following hypotheses: 1) the fluid flow takes place in the laminar range, 2) the cubic law is locally valid at the fracture cell's scale. The hydraulic conductivity between cells i and j is calculated as harmonic mean. The volumetric flow rate Q_{ij} between cells i and j with apertures a_i and a_j, respectively, is then proportional to the hydraulic head gradient, as follows:

$$Q_{ij} = \frac{g}{12\nu} \frac{2\Delta e}{\left(\frac{1}{a_i^3} + \frac{1}{a_j^3}\right)} \left(\frac{h_i - h_j}{\Delta e}\right) \tag{3}$$

where $g\,[m/s^2]$ denotes gravitational acceleration, $\nu[m^2/s]$ is kinematic viscosity and h_i and h_j are hydraulic heads at cells i and j, respectively.

In a steady-state flow condition, the principle of mass conservation at node i connecting to other nodes j can be written as the following equation:

$$\sum_j Q_{ij} = 0 \tag{4}$$

After prescribed unit hydraulic heads at two opposite boundaries (Figure 3), Eq. (4) can be solved for the global flow in a single fracture. No flow

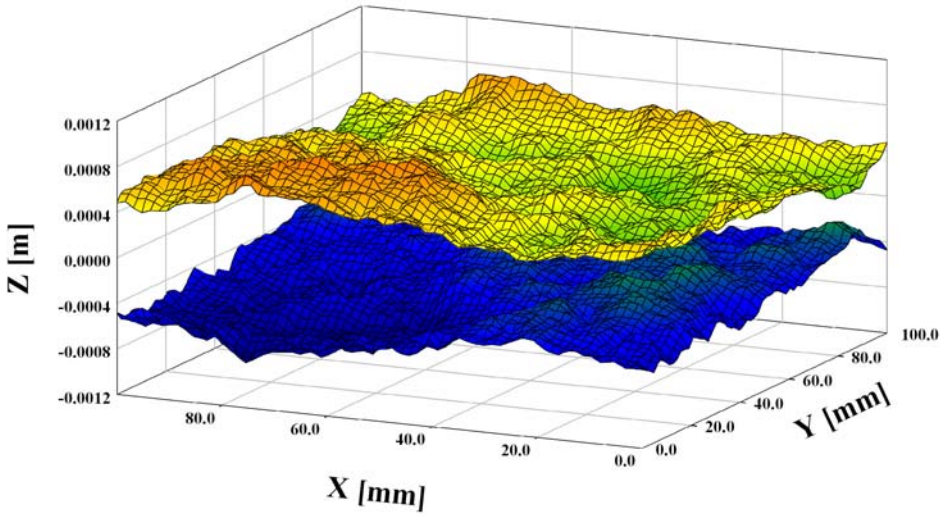

Figure 2. A rough fracture generated by two fractal surfaces (D = 2.5).

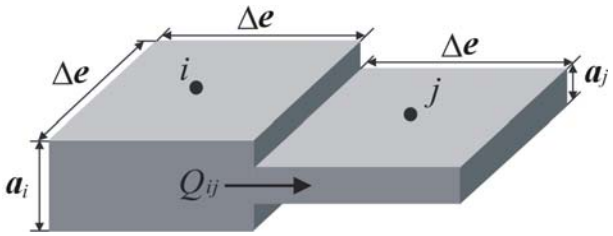

Figure 3. Schematic illustration of fluid flow through a rough single fracture.

condition is imposed at two boundaries parallel to the flow direction.

A five-point finite difference scheme using an iterative preconditioning conjugate gradient method is adopted to solve a system of linear equations from Eq. (4) (Ciarlet, 1983). The solution of this system yields the hydraulic head at each node, except for the nodes at the left and right boundaries. The volumetric flow rate between adjacent nodes is then calculated by using Eq. (3).

Figure 4 shows the distributions of volumetric flow rate in the single fracture of $D = 2.5$ with two different values of mean aperture of (a) $a = 0.425mm$ and (b) $a = 0.209mm$. It can be observed that when the mean aperture is diminished, the channeling effect for the flow becomes more apparent because of increment of contact areas.

2.3 Transport model

The classical three-dimensional random walk model, which is expressed by Eq. (5), is used to simulate the solute transport in this study (Kinzelbach, 1986):

$$X^j = \sum_{i=0}^{n-1} \left[u_X^j(Z^j)dt + \delta\xi_{i,D_m}^X \right]$$
$$Y^j = \sum_{i=0}^{n-1} \left[u_Y^i dt + \delta\xi_{i,D_m}^Y \right] \quad (5)$$
$$Z^j = \sum_{i=0}^{n-1} \left(\delta\xi_{i,D_m}^Z \right)$$

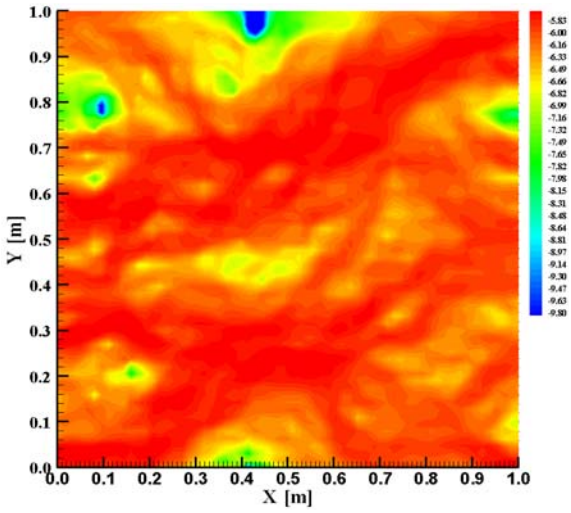

(a)

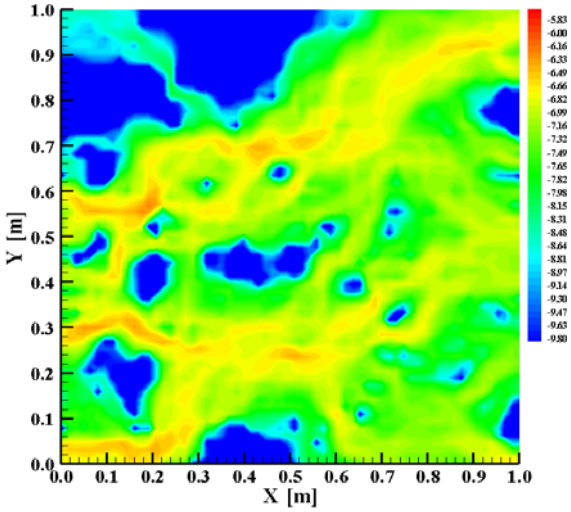

(b)

Figure 4. Distributions of volumetric flow rate in the single fracture of *D=2.5* with two different apertures of (a) a=0.4mm and (b) a=0.2mm. Blue areas represents the contact zones. In the figures above, the local flow rates are represented as the log scale.

where X^j, Y^j and Z^j are the positions of particle j in X, Y and Z directions, u_X and u_Y are the velocities of X and Y directions, n is the particle numers and $\delta\xi_{i,D_m}$ is the random number extracted from the law of normal distribution with mean of zero and standard deviation of $\sqrt{2D_m dt}$. D_m can be calculated independently for each particle according to its diameter and by the bias of Stoke-Einstein equation.

In this study, we developed a new transport model which is based on the equations (Eq. 5) and can be able to simulate the transport behavior of solutes according to the variation of particle size.

3. Transport simulations

3.1 Effect of fracture roughness variation

In this section, the dispersion of particles according to the variation of fracture roughness is investigated. The four rough fractures of $D = 2.0,\ 2.3,\ 2.5$ and 2.9 are generated. For the upper and lower fractal surfaces, the mean of $0.1mm$ and standard deviation of $0.05mm$ are simultaneously used and the mean aperture is $0.5mm$ for three different fractures.

Figure 5 represents the results of transport simulations according to the fractal dimension (fracture roughness). Generally, more the fractal dimension increases, more the fracture is rough (Figure 6). With the increasing fractal dimension, the mean residence time is much faster and the particle clouds is more dispersed (Figure 5).

Figure 7 represents the evolution of the longitudinal dispersion coefficient with time for four different fractal dimensions. It can be identified that in the case of the smoothest fracture ($D = 2.0$), the coefficient of longitudinal dispersion is arrived very quickly at the asymptotic regime (the theoretical asymptotic regime

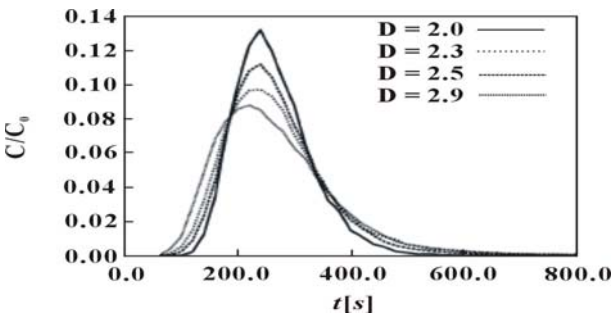

Figure 5. Variation of breakthrough curves according to the fracture roughness.

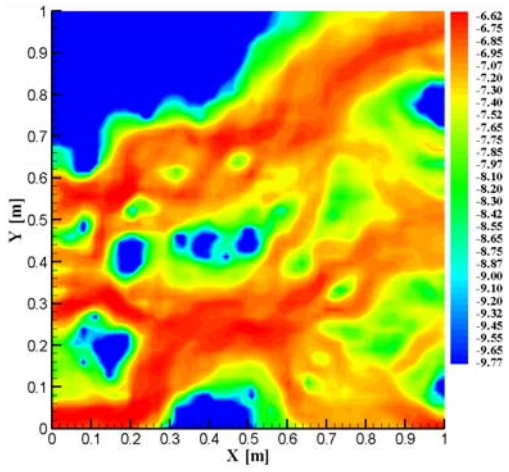

(a)

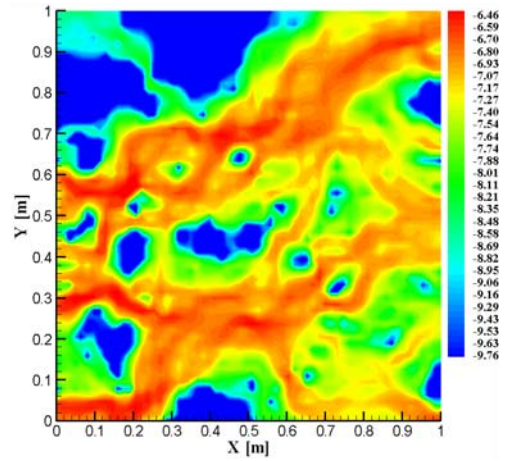

(b)

Figure 6. Volumetric flow rate distribution according to the fractal dimension (D) ((a) $D = 2.3$ and (b) $D = 2.5$).

(Eq. 1) is represented by a dotted line in Figure 7). For the fracture of $D = 2.3$, the asymptotic regime is attained but less quickly than the case of fracture of $D = 2.0$. For the more rough fractures ($D = 2.5$ and 2.9), the molecular diffusion does not have enough time to homogenize particles in the aperture and the asymptotic regime is not reached yet. This phenomenon has been observed by Grindrod and Lee (1996) and Wels et al. (1997). In general, when the fractal dimension increases, the velocity field in the rough fracture is perturbed and then more heterogenous: finally, the dispersion of particles displaced in the rough fracture increases.

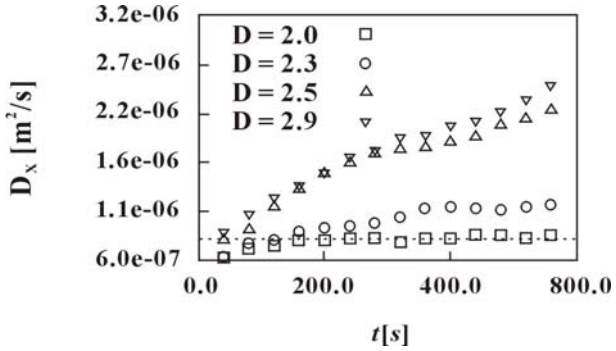

Figure 7. Variation of longitudinal dispersion according to the fracture roughness.Figure 7.

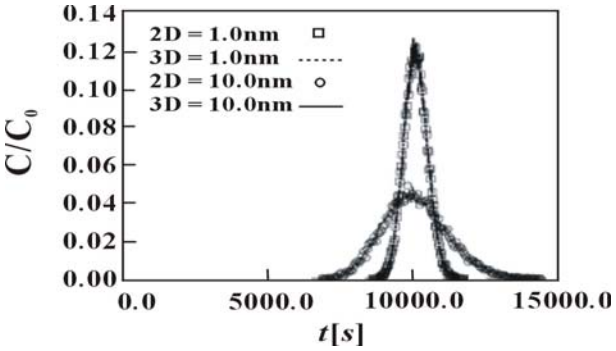

Figure 8. Comparison of breakthrough curves between 2D and 3D transport models for two different particle size of 1.0 and 10.0nm.

Table 1. Summary of data used in the simulation

Fracture size	10cm × 2.2cm
Fracture aperture	0.5mm(uniform)
Particle size (nm)	1
	10
	100
	1000

3.2 Effect of particle size variation

3.2.1 Single-sized particles

This transport simulation was carried out with four different sizes of particles: 1, 10, 100 and 1000nm. The particles are displaced in a smooth fracture with a length of 10cm and a width of 2.2cm, respectively. In this study, the 3D smooth fracture model was used and the aperture was constant as 0.5mm.

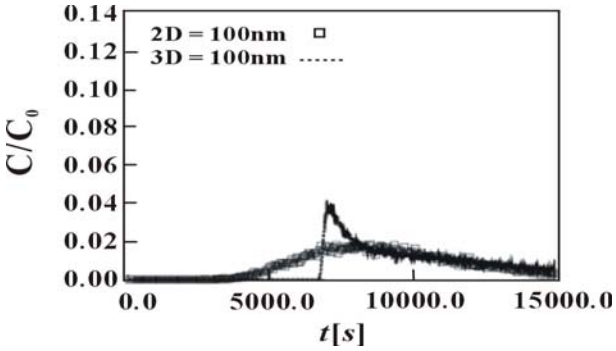

Figure 9. Comparison of breakthrough curves between 2D and 3D transport models for particle size of 100.0nm.

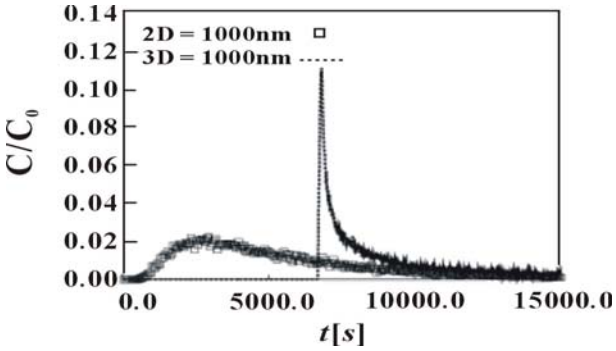

Figure 10. Comparison of breakthrough curves between 2D and 3D transport models for particle size of 1000.0nm.

Table 2. Results of transport simulation from 2D and 3D transport models for four different particle sizes.

Radius (nm)	D_m (m^2/s)	Critical time (s)	D_X^{2D} (m^2/s)	D_X^{3D} (m^2/s)
1	1.87×10^{-10}	812.0	8.23×10^{-10}	8.23×10^{-10}
10	1.87×10^{-11}	8127.0	6.38×10^{-9}	6.38×10^{-9}
100	1.87×10^{-12}	81273.0	6.36×10^{-8}	4.30×10^{-8}
1000	1.87×10^{-13}	812736.0	6.36×10^{-7}	8.64×10^{-7}

Table 2 represents the results simulated from 2D and 3D transport models for four different particle sizes. The breakthrough curves for each particle size are presented in Figures 8 (1 and 10nm), 9 (100nm) and 10 (1000nm) and in each figure, the results from 2D and 3D transport model were compared.

It can be observed that for small particle sizes (1 and 10nm), the breakthrough curves between 2D and 3D transport models were almost identical. In figure 8, it is shown that the mean residence times from both 2D and 3D transport simulations are bigger

than the critical time. For these cases, the dispersion of Taylor-Aris of Eq. (1) can be applied to simulate the particle transport in the fracture.

However, for the particles of 100nm and 1000nm, the mean residence times are smaller than the critical time. The molecular diffusion does not have enough time to homogenize the particles in the fracture. In these cases, the dispersion of Taylor-Aris cannot be then adopted.

The 2D transport model supposes that the first arrival time of particles is very short because the coefficient of dispersion of Taylor-Aris increases according to the particles' size. This result can be derived from the fact that the mean velocity U is calculated between $-\left(\frac{a}{2}-r\right)$ and $\left(\frac{a}{2}-r\right)$, where r is the radius of a particle. This mean velocity is thus bigger than that calculated between $-\frac{a}{2}$ and $\frac{a}{2}$.

The 3D model, which reflects the more microscopic and more physical processes (molecular diffusion and velocity profile of Poiseuille's type in the fracture), considers the particles which are displaced slower than the maximal velocity of the fracture $\left(\frac{3U}{2}\right)$. The theoretical arrival time of particles is $\frac{2L}{3U}$ and the calculated value is thus of 6666.6s. This arrival time corresponds to that calculated numerically in these simulation (Figure 11 and 12). This difference between 2D and 3D transport models induces the different coefficients of dispersion. As consequence, it can be identified that as shown in Table 1, the 2D transport model has a tendency to overestimate the dispersion and this tendency is more apparent according to increasing particles' size.

3.2.2 Multi-sized particles

In these simulations, the 3D transport model is used because this model is able to consider the variabilityof particle size and the parabolic velocity profile as well as the molecular diffusion.

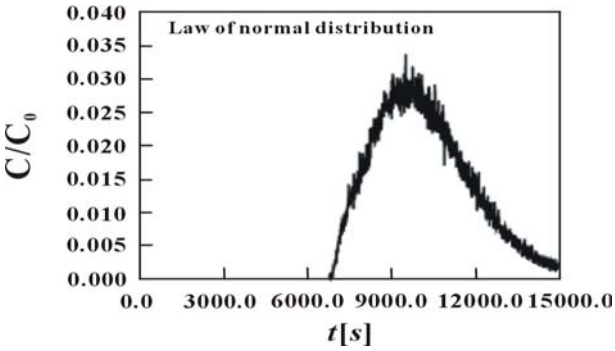

Figure 11. Breakthrough curves from the law of normal distribution of particles' radii.

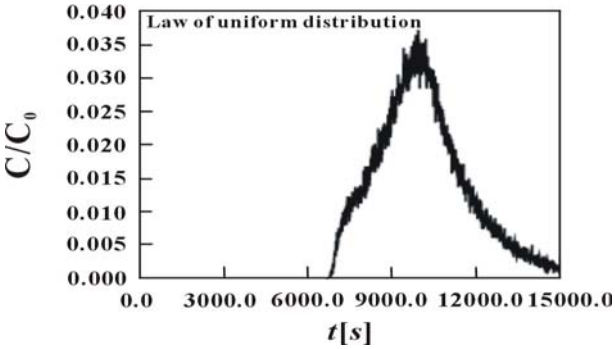

Figure 12. Breakthrough curves from the law of uniform distribution of particles' radii.

The radii of particles are distributed by using two simple laws: uniform and normal (or Gaussian) distribution laws. The coefficients of molecular diffusion are thus calculated with these radii by the bias of the Stoke-Einstein formula. Each particle has its radius and coefficient of molecular diffusion. These radius and coefficient are used to consider the boundary condition and the diffusion process, respectively.

Figures 11 and 12 show the results of transport simulations and the breakthrough curves reflects the influence of the heterogeneity of particle size in the fracture. There is not the apparent difference between two breakthrough curves from the normal and uniform distribution laws. It seems that the standard deviation applied to the normal distribution law is not enough to influence the transport. However, the uniform distribution law imposes an equiprobability of particles' radii between 1 and

100nm and gives a breakthrough curve deformed by the coexistence of very small and very big particles. These results agrees well with those by James and Chrysikopoulos (1999) and Wels et al. (1996).

4. Conclusion

In this study, the 3D transport model based on the random walk technique was developed to simulate the solute transport in a rough fracture. The summary of the results obtained from the transport simulations is as follows:

1. The choice of the 2D and 3D transport models is important according to the given transport problems (e.g. particle size, etc.).

2. When the roughness of the fracture increases, the particles arrive thus more quickly and the dispersion of particles increases.
3. When the laws of distribution of particles' radii are introduced, it can be shown that the breakthrough curves are very different with those in the case of the uniform size of particles. The heterogeneity of the particle size influences thus the solute transport.

4. The particles of larger size were collected more quickly at the lower boundary and their dynamic dispersion was thus larger.

5. When the heterogeneity of particle size (that is, the standard deviation of particle size) increases, the dispersion of the solute increases.

We can expect that the transport model developed in this study will be applied to analyze the transport behavior of various solutes such as radioactive substances which may be generated from the radioactive waste disposal system.

(접수일 : 2006. 8. 8 심사일 : 2006. 8. 14 심사완료일 : 2006. 9. 7)

REFERENCES

1. Aris R.(1956), On the dispersion of a solute in a fluid flowing through a tube, *Proc. Roy. Soc. London*, A 235, pp. 67~77.
2. Brown S. R.(1995), Simple mathematical model of rough fracture, *J. Geophys. Res.*, B 100 (4), pp. 5941~5952.
3. Ciarlet, P.(1983), Introduction de l'analyse numérique matriciel et de l'optimisation, Masson.
4. Grindrod P. and Lee A. J.(1996), *Colloid migration in non-uniform fractures: particle tracking in 3D,* Technical report, INTERA, United Kindom.
5. Fleurant C.(200), *Modélisation stochastique du transport de mass dans les milieux poreux et fracturés*, Thèse, Ecole Nationale Superieure des Mines de Paris.
6. Hull L. C., Miller J. D., Clemo T. M.(1987), Laboratory and simulation studies of solute transport in fracture networks, *Water Resour. Res.*, Vol. 23, No. 8, pp. 1505~1513.
7. James S. C. and Chrysikopoulos C. V.(1999), Transport of poly-disperse colloid suspensions in a single fracture, *Water Resour. Res.*, Vol. 35, No. 3, pp. 707~718
8. Jeong W. C.(2000), *Modelisation de l'influence d'une zone de faille sur l'hydrogeologie d'une milieu fracturé*, Thèse, Ecole des Mines de Paris.
9. Kessler J. H. and Hunt J. R.(1994), Dissolved and colloidal contaminant transport in a partially clogged fracture, *Water Resour. Res.*, Vol. 30, No. 4, pp. 1195~1206.

10. Kinzelbach W.(1986), *Groundwater modelling*, Elsevier.
11. Neretnieks I., Erikse T. and Tähtinen P.(1982), Tracer movement in a single fracture in granitic rock: some experimental results and their interpretation, *Water Resour. Res.*, Vol. 18, No. 4, pp. 849~858.
12. Novakowski K. S., Evans G. V., Lever D. A. and Raven K. G.(1985), Example of measuring hydrodynamic dispersion in a single fracture, *Water Resour. Res.,* Vol. 21, No. 8, pp. 1165~1174..
13. Wels C., Smith L. and Vandergraaf T. T.(1996), Influence of specific surface area on transport of sorbing solutes in fractures: an experimental analysis, *Water Resour. Res.*, Vol. 32, No. 7, pp. 1943~1954.
14. Wels C., Smith L. and Beckie R.(1997), The influence of surface sorption on dispersion in parallel plate fractures, *J. of Contam. Hydrol.*, Vol. 28, pp. 94~114.